Indian Journal of Chemical Technology
Vol. 29, March 2022, pp. 201-206

Corrosion inhibition, adsorption behaviour, and thermodynamic studies of red dragon fruit (*Selenicereus costaricensis*) waste peel extracts on mild steel in acidic environment

Romulo R Macadangdang Jr.
College of Allied Health, National University, Manila, Philippines
E-mail: rjrsmacadangdang@national-u.edu.ph

Received 23 January 2022; accepted 26 February 2022

Metal corrosion is brought about by the oxidation of atoms on the surface resulting in irreversible damage to structures at staggering costs. Hence, the search for efficient and cost-effective corrosion inhibitors is relevant. In this study, the ethanolic extract of Red Dragon Fruit (*Selenicereus costaricensis)* waste peels (RDF) has been tested for its anti-corrosion property using the weight loss method at different temperatures (303-343 K). The calculated inhibition efficiency of 2% RDF is 97%. Thermodynamic studies reveal that increasing inhibitor concentration raises the activation parameters of mild steel in acidic media such as activation energy (E_a) and changes in enthalpy (ΔH^o) and entropy (ΔS^o). Moreover, increased immersion time, inhibitor concentration, and temperature led to increased inhibition efficiency. The spontaneous process (ΔG^o_{ads} = -23.47 kJ/mol) of adsorption of RDF on mild steel surfaces obeys the Langmuir isotherm model. Lastly, optical microscopy of the inhibited and uninhibited systems confirms the potential of the RDF against pitting corrosion.

Keywords: Corrosion, Corrosion inhibition, Adsorption, Thermodynamic studies, weight loss method, Environment-benign coatings

Corrosion is characterized by the degeneration of surfaces in a particular environment or condition[1]. In fact, corrosion imposes a worldwide problem where everyone is concerned because it directly affects the big and small companies and economy of countries. This chemical reaction is a combination of oxidation and reduction processes and has various detrimental effects in infrastructure, resources and art and comes with serious financial implications. Metals, such as mild steel, are of huge value in the industry, whether small-scale or large-scale, and in the household. However, when mild steel is exposed to atmospheric oxygen and numerous gases and chemicals, it tends to corrode which leads to contamination, safety issues and reduction in efficiency[2]. The latter is just an example wherein metal, a non-renewable resource, is wasted which can even lead to the scarcity of metal someday. The need for low-cost, environment-friendly, and efficient corrosion inhibitor should be addressed.

Since corrosion is a natural phenomenon, metals will just corrode over time, especially if they are left without any maintenance, preventive coatings, or corrosion inhibitors. Several corrosion inhibitors such as novel triazole derivatives[3], Schiff base compounds[4], alkylimidazolium ionic liquids[5], and macrocylic polyether compounds[6], plant extracts[7-10] have been reported. Among these known corrosion inhibitors, particular interest is pointed to plant extracts as these require facile and green extraction processes.

Selenicereus contaricensis, locally known as red dragon fruit (RDF) has peels characterized by bright red color and no food value. The bright red pigment in RDF was reported to contain rich phytochemicals such as anthocyanins[11], flavonoids and polyphenols[12] which are known antioxidants. In theory, antioxidants impede the oxidation reaction making this group an excellent choice for corrosion inhibition.

Hence, the goal of this study is to explore the potential of Red Dragon Fruit (RDF) peel ethanolic extract as a corrosion inhibitor for mild steel that was submerged in acidic medium (1M HCl). The corrosion inhibition efficiency and corrosion rate were probed by mass loss measurements. A morphological assessment of mild steel products was done using optical microscopy to compare the surface of bare mild steel coupons and their coated counterparts. In addition, this study also aims to elucidate the thermodynamics and adsorption behavior of the adsorption and corrosion inhibition processes.

Experimental Section

Inhibitor preparation, authentication

Selenicereus costaricensis was collected from the Burgos, Ilocos Norte, Philippines. Voucher specimens were sent to the National Museum of the Philippines for verification and authentication. The extraction protocol was based from a study elsewhere with slight modification[13]. The peels were manually separated, dried, and then pulverized using a blender. Thereafter, 100 g powdered peels were subjected to reflux in 1.0 M HCl solution for the next 4h and kept for additional 10h. The stock solution (10% v/v) was prepared from the afforded filtrate of the extract. Furthermore, test solutions ranging from 0.05% to 2% v/v concentration were prepared from the stock solution after further dilution with the correct quantity 1.0 M HCl.

Preparation of specimen

Mild steel specimens of size 1.0 × 5.0 × 0.5 cm^3 were polished with 400 and 600 grade emery paper, degreased with acetone in a sonic bath, washed with deionized water (Ultrapure Milli-Q), dried and kept in a desiccator for the experimental study.

Mass loss measurements

In separate containers, pre-weighed mild steel samples were suspended in 120 mL of 1.0 M HCl solutions containing different inhibitor concentrations and the controls with the aid of glass hook at various immersion periods such as 1, 4, 7, and 24h at room temperature[13]. The samples were then removed, washed with deionized water, dried, and reweighed after specified time of immersion.

The inhibition efficiency (IE%) was calculated as percentage using Equation 1:

$$IE\% = \frac{(W_0 - W_x)}{W_x} 100\% \quad \ldots (1)$$

where W_0 is the weight loss (in mg) of metal without RDF inhibitor and $W_x$is the weight loss (in mg) of metal with RDF inhibitor[9].

Further, the rate of corrosion (R_C) was calculated using Equation 2:

$$R_C = \frac{\Delta W}{At} \quad \ldots (2)$$

where ΔW is the change in weight (mg), A is the exposed area (cm^2), and t corresponds to the exposure time (h)[9].

To explore the thermodynamics of the process, same methodology was applied at elevated temperatures (303K-343K) keeping the immersion time constant at 1h. All measurements were done in triplicates and the values that appear henceforth are the reported means[14].

Surface examination studies

Surface analysis of mild steel specimens was done to study the changes that occurred during the corrosion of mild steel in the absence and presence of inhibitors. The inhibitive action of plant extracts on mild steel corrosion was investigated by Optical Microscope technique. The micrographs of the uninhibited and inhibited specimens were obtained which aided the examination of the nature of corrosion product formed on the surface of mild steel samples. The micrographs were compared in terms of the amount of visible amount of corrosion, such as the amount of orange-to-reddish brown streaks and amount of pitting involved.

Statistical analysis

Statistical Package for the Social Sciences (SPSS) 27.0 was used for the data analysis of this study. The data collected were tested using two-way analysis of variance (ANOVA) as there were two parameters in the study–immersion time and concentration. It was used to determine if there are any significant differences (α=0.05) between the different set-ups. In this way, the level of significance was found and determined whether the extract could lessen the rate of corrosion in mild steel.

Results and Discussion

Mass loss measurements

Effect of concentration

Owing to the simplicity of method and high reliability, the weight loss method was employed to monitor the corrosion rate of mild steel in acidic medium in the presence and absence of red dragon fruit peels extract as inhibitor. Moreover, the mass loss method was also used to estimate the inhibition efficiency of the RDF at varying concentrations. Figure 1 depicts the relationship of inhibitor concentration (% v/v) with corrosion rate (mg/cm^2h) and inhibition efficiency (IE%). With an increase in RDF inhibitor concentration from 0.05% to 2%, the corrosion rate followed a downward trend while improved inhibition efficiency was observed. This result signals that adsorbed RDF particles on to the surface of mild steel specimens served as protecting stratum[15,16].

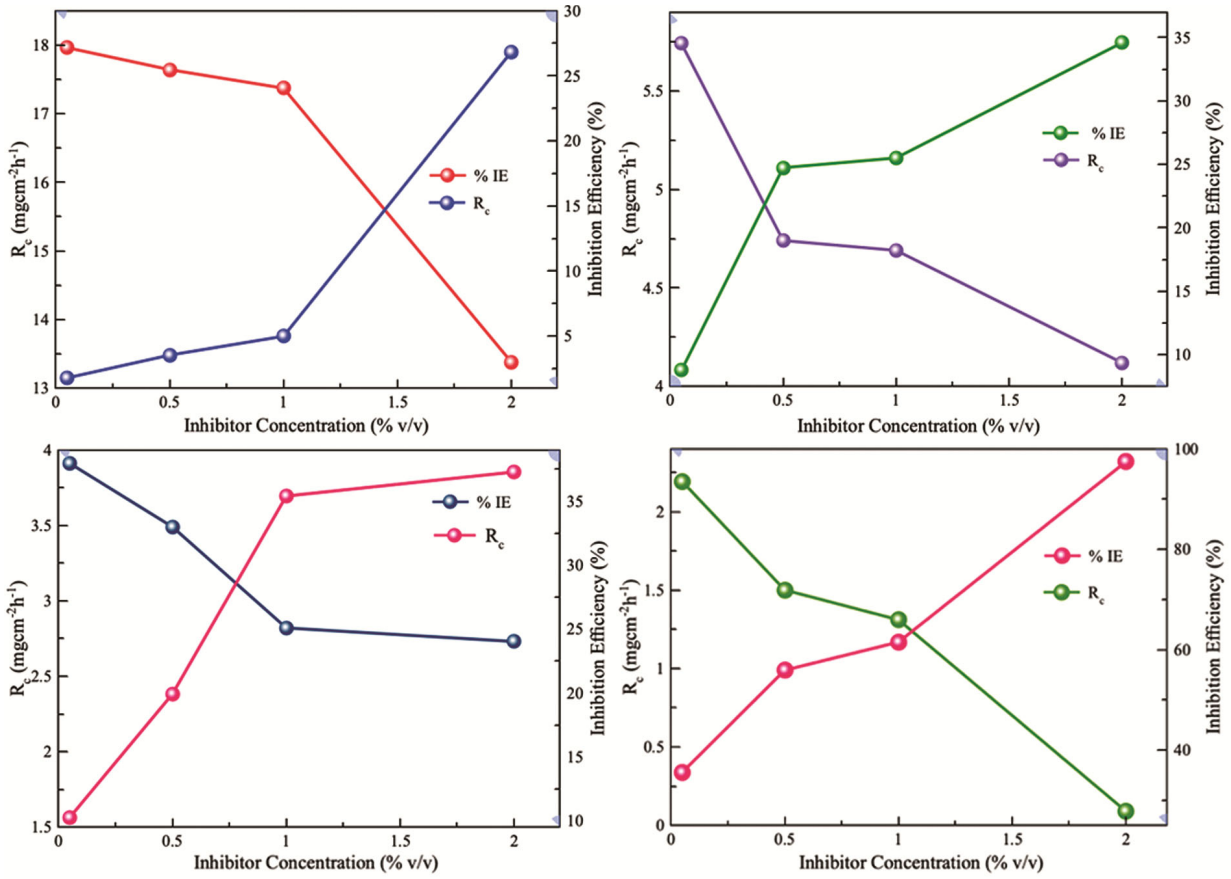

Fig. 1 — Corrosion rate and inhibition efficiency as a function of concentration at different immersion time

Effect of immersion time

At constant temperature, the effect of immersion time from 1h up to 24h was investigated. Table 1 suggests that increasing immersion time leads to enhanced inhibition efficiency and lower corrosion rate. The highest value for inhibition efficiency, 97.41% was charted at 2.0% RDF loading at 24 hours. This suggests that longer immersion time allows the constituents of RDF to fully saturate the surface of mild steel thus, providing an efficient protective barrier against corrosion. For the adsorption of RDF extracts on mild steel in this study, no significant signs of desorption were detected contrary to previously reported literature where deterioration of inhibition efficiency was observed [17].

Effect of temperature

To probe the thermodynamics and stability of the adsorption process of RDF on mild steel, similar protocols were performed as above, but with temperature variation from 30°C to 70°C at a constant immersion time (24h) as summarized in Table 2. A marked rise in the rate of corrosion was observed with

Table 1 — Effect of immersion time at constant temperature

RDFConc (% v/v)	Immersion time (h)							
	1		4		7		24	
	R_C	IE	R_C	IE	R_C	IE	R_C	IE
Blank	18.29		6.30		4.36		3.39	
0.050	17.96	1.79	5.74	8.76	3.91	10.27	2.19	35.55
0.50	17.64	3.54	4.74	24.73	3.49	19.90	1.50	55.87
1.0	17.37	4.99	4.69	25.50	2.82	35.39	1.31	61.51
2.0	13.38	26.83	4.12	34.58	3.25	37.27	0.09	97.41

T = 27°C | R_C = mgcm^{-2}h^{-1} | IE = %

Table 2 — Effect of various temperatures on mild steel corrosion in acidic environment

RDF Conc (% v/v)	Temperature (K)				
	303	313	323	333	343
Blank	5.65	7.17	9.48	12.56	20.50
0.050	5.57	7.03	9.13	11.96	15.13
0.50	5.39	6.76	9.24	11.75	15.08
1.0	5.26	6.55	9.01	1159	14.99
2.0	4.21	5.83	8.57	11.36	13.92

Immersion time = 24h | R_C = mgcm^{-2}h^{-1} | IE = %

increasing temperature especially in the unprotected surface of the blank. Meanwhile, corrosion rate slowed down with higher % RDF extract concentration even at elevated temperatures. It is apparent that the presence of RDF constituents on the mild steel surface prevented the disbanding of metal from the bulk sample and this may be due to the formation of iron-RDF complex layer via physical sorption[18]. The effect of temperature on corrosion rate as a function of inhibitor concentration is presented in Fig. 2.

Determination of activation and thermodynamic parameters

The mechanism of corrosion inhibition is revealed through determination of the activation energy by changing the temperature in the presence and absence of inhibitors. Using the Arrhenius equation,

$$R_C = Ae^{\left(\frac{-E_a}{RT}\right)} \quad \ldots (3)$$

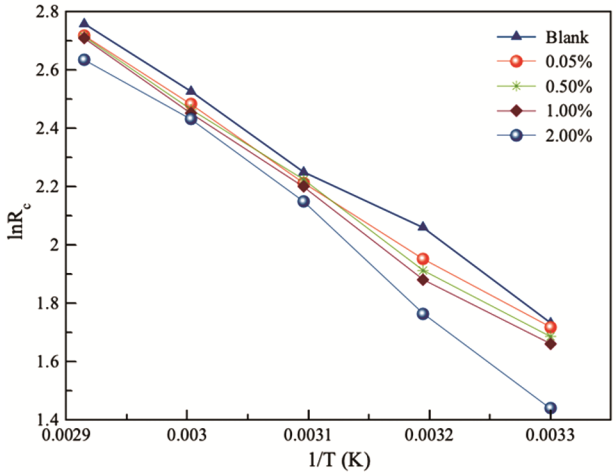

Fig. 2 — Arrhenius plot for the effect of temperature

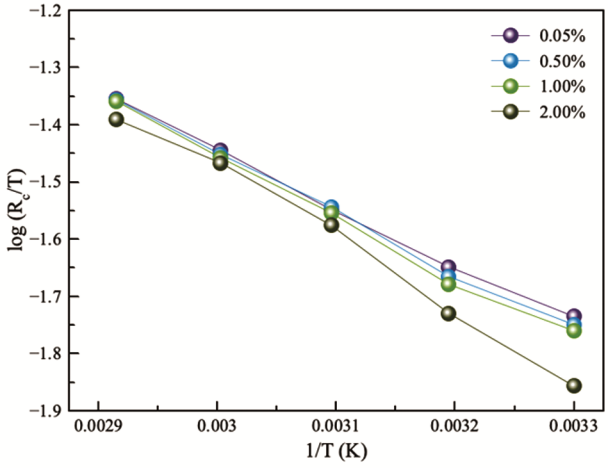

Fig. 3 — Alternative Arrhenius plot for mild steel in aqueous medium in the absence and presence of different concentrations of RDF extract

where R_C is the corrosion rate, Ea is the activation energy, T is the temperature in Kelvin, A is the Arrhenius pre-exponential constant, and R is the universal gas constant (8.314 $Jmol^{-1}K^{-1}$), a plot of $ln\mathrm{R_C}$ as function of inverse temperature ($1/T$) allows the estimation of activation energy (Fig. 3). The activation energy of the uninhibited system was lower compared to inhibited systems signifying slower rate of corrosion as summarized in Table 3. Due to the accumulation of RDF constituents on to the surface of the substrate, higher energy barrier must be exceeded to bring about corrosion[19,20].

Other thermodynamic parameters such as standard enthalpy of activation and standard entropy of activation were also calculated from the results of temperature variation studies using the transition state equation,

$$R_C = \frac{RT}{N_A h} e^{\left(\frac{-\Delta H^o}{RT}\right)} e^{\left(\frac{\Delta S^o}{R}\right)} \quad \ldots (4)$$

where N_A is Avogadro's number and h is Planck's constant. The slopes and intercepts of the graphs presented in Fig. 3 allowed the calculation of these thermodynamic parameters.

Other thermodynamic parameters are presented in Table 4. The calculated values for the enthalpy of activation ranges from 18.73 to 23.83 $kJmol^{-1}$ indicate an endothermic and physical adsorption process. Meanwhile, the negative values for the entropy of activation strongly suggest a non-spontaneous phenomenon in the case of adsorption of RDF onto the surface of the mild steel. This suggests the associative formation of RDF-MS complex hence a decline in disorder[21].

Adsorption Isotherm

Studies on adsorption isotherms were performed to further grasp the interaction of RDF inhibitor and

Table 3 — Values of activation parameters obtained for MS in 1M HCl solution at various concentration of inhibitor

	RDF concentration (% v/v)				
	Blank	0.05%	0.50%	1.00%	2.00%
slope	-2619.8	-2626.8	-2711.0	-2767.8	-3187.6
E_a ($kJ\ mol^{-1}$)	21.78	21.84	22.54	23.01	26.50
r^2	0.9961	0.9976	0.9971	0.9900	0.9938

Table 4— Standard enthalpy and standard entropy of the adsorption of RDF on mild steel

	RDF concentration (% v/v)				
	Blank	0.05%	0.50%	1.00%	2.00%
ΔH^o ($KJmol^{-1}$)	18.73	19.16	19.87	20.33	23.83
ΔS^o ($Jmol^{-1}K^{-1}$)	-180.20	-167.74	-165.68	-164.41	-154.38

the mild steel substrates. The surface coverage parameter (Θ) for different concentrations of RDF was calculated from the weight loss data. Graphical testing was used to find an appropriate adsorption isotherm. A plot of C/Θ as a function of concentration was generated to afford the data presented in Fig. 4. The graphs show linear slopes conforming to the Langmuir model ($r^2 \cong 1$) at immersion times greater than 4h. Moreover, this result confirms that 1hr immersion time was not enough for RDF to saturate the surface of the substrate. Immersing the system in 4h and 7h showed high linearity, however, the 24h immersion time yielded a value closest to unity (0.9984). This means that 24 h is the most appropriate immersion time allowing RDF constituents to fully adsorb on the exposed surfaces of the mild steel samples.

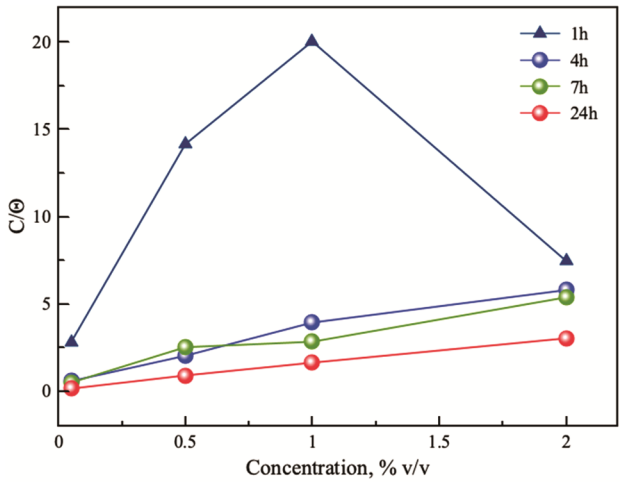

Fig. 4 — Langmuir isotherm plots of MS in 1 M HCl at different concentration s of inhibitors

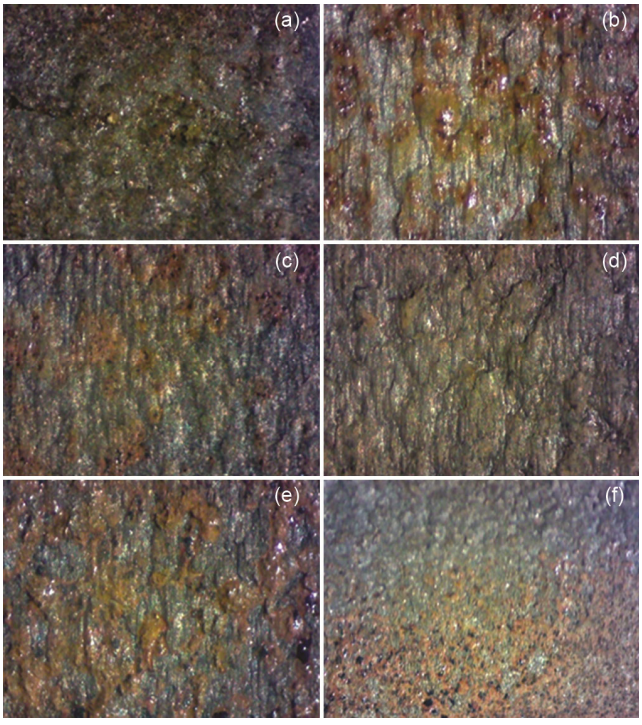

Fig. 5 — Optical micrographs for uninhibited and inhibited mild steel soaked in 1M HCl

The standard free energy of adsorption (ΔG_{ads}) calculated using the equation,

$$\Delta G_{ads} = -RT \ln(K_{ads} x A) \quad \ldots (5)$$

where, R is the gas constant (8.314 $Jmol^{-1}K^{-1}$), K_{ads} is the equilibrium constant for adsorption, T is the temperature (300 K) and A is water density. Table 5 summarizes the computed values of the ΔG_{ads} and K_{ads}. For the curves that obey the Langmuir isotherm, the calculated values for the standard free energy range from -23.47 to -20.56 $kJmol^{-1}$, which is typical of physisorption[22]. Therefore, the adsorption of RDF extract on the surface of mild steel did not involve electron sharing to afford a chemical bond[23,24].

Surface examination studies

The specimens were also studied under an optical microscope with two light sources. The images for the different set-ups are shown in Fig. 5.

Figures 5a shows an image of the corroded surface of the metal sample from the treatment containing 0.05% dragon fruit extract. The micrograph of the representative metal samples from the other three treatments, specifically the treatments containing 0.50%, 1.00%, and 2.00% dragon fruit extract, are also depicted in Figs. 5b, 5c, and 5d, respectively. In addition, micrographs were also taken for the surface examination studies of the negative and positive control (WD-40) setups, as shown in Figs 5e and 5f, respectively.

The pictures obtained from optical microscopy showed the amount of corrosion for each of the set-ups.

Table 5 — Equilibrium constant and standard Gibbs energy for RDF adsorption

Immersion time (h)	Mass loss measurements				
	Slope	Y-intercept	r^2	ln K_{ads}	ΔG (kJ mol^{-1})
1	1.2949	9.9542	0.0206	0.1300	-12.14
4	2.6712	0.704	0.9715	3.794	-20.56
7	2.3341	0.726	0.9529	3.215	-20.14
24	1.4652	0.1201	0.9984	12.20	-23.47

T = 27°C

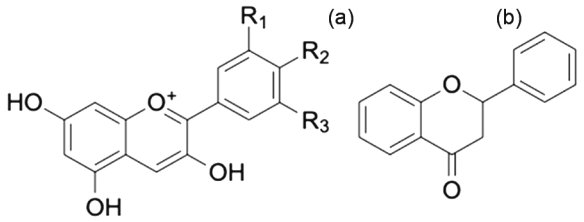

Fig. 6 — General structures for (A) anthocyanins and (B) flavonoids

The brownish orange streaks in the picture show the deposits of hydrated iron (II) oxide. The microscopy also revealed that the type of corrosion that occurred is pitting corrosion. Moreover, it confirms that the increase in the amount of RDF extract reduces a significant amount of corrosion that can happen on the surface of mild steel, since the amount of brownish orange streaks decreased visibly. Furthermore, negative control, comprised of HCl only, showed the most corrosion and contains more pits on the surface.

Mechanism of inhibition

RDF extracts were previously reported to phytochemicals with high antioxidant activities such as anthocyanins, polyphenols, and lavonoids[10,12,25-28]. A common motif to these phytochemicals are chromophores and the presence of oxygen-heteroatom in the ring structures which ramps up their adsorptive ability on mild steel surface (Fig. 6). The pi-electrons and lone pairs from the RDF constituents effectively associate with the unfilled d-orbital of iron and hence, serve as sites of adsorption. As seen from the thermodynamic values obtained in the present study, these organic molecule components are adsorbed physically forming a protective envelope and thus explains their inhibitory activity against corrosion brought about by aggressive electrolytes.

Conclusion

Corrosion inhibition of RDF on mild steel exposed in acidic medium has been examined in the present study. Inhibition efficiency increases with RDF concentration and immersion time with maximum efficiency of 97% reached for 2.00% waste peel extract in 24h. Corrosion rate declined with increased RDF concentration but increased with temperature. Activation energy for the corrosion process increases with concentration due to the physisorption of RDF on to the metal surface. The adsorption process is found spontaneous and obeys the Langmuir isotherm model. Surface examination of the specimen reveal pitting corrosion in uninhibited samples, while the inhibited specimens showed little signs of oxidation. Overall, the results confirm the effectiveness of RDF as corrosion inhibitor.

References

1 Sedik A, Lerari D, Salci A, Athmani S, Bachari K, Gecibesler İ H & Solmaz R, *J Taiwan Inst Chem Eng*, 107 (2020) 189.
2 Prasad A R, Kunyankandy A & Joseph A, *Corrosion Inhibitors in the Oil and Gas Industry*, Saji V S & Umoren S A, Wiley-VCH Verlag Gmb H & Co. KGaA, Weinheim, Germany (2020) 135.
3 Nahlé A, Salim R, E l Hajjaji F, Aouad M R, Messali M, Ech-Chihbi E, Hammouti B & Taleb M, *RSC Adv*, 11 (2021) 4147.
4 Al-Amiery A, Salman T A, Alazawi K F, Shaker L M, Kadhum A A & Takriff M S, *Int J Low Carbon Technol*, 15 (2020) 202.
5 Hajjaji F E, Salim R, Taleb M, Benhiba F, Rezki N, Chauhan D S & Quraishi M A, *Surf Interf*, 22 (2021) 100881.
6 Paul P K, Yadav M & Obot I B, *New J Chem*, 45 (2021) 6826.
7 Akinbulumo O A, Odejobi O J & Odekanle E L, *Results Mater*, 5 (2020) 100074.
8 Dehghani A, Bahlakeh G, Ramezanzadeh B & Ramezanzadeh M, *Constr Build Mater*, 245 (2020) 118464.
9 Ogunleye O O, Arinkoola A O, Eletta O A, Agbede O O, Osho Y A, Morakinyo A F & Hamed J O, *Heliyon*, 6 (2020) 03205.
10 Haque J, Verma C, Srivastava V & Nik W W, *Sustain Chem Pharm*, 19 (2021) 100354.
11 Rosiana N M, Suryana A L & Olivia Z, *Earth Environ Sci*,672 (2021) 012055.
12 Padmavathy K, Sivakumari K, Karthika S, Rajesh S & Ashok K, *Int J Pharm Sci Res*, 12 (2021) 2770.
13 Rosli N R, Yusuf S M, Sauki A & Razali W M, *Key Engineering Materials*, Trans Tech Publications Ltd. Freienbach, Switzerland, 797 (2019) 230.
14 Kavitha N, Kathiravan S, Jyothi S, Murugesh A & Ravichandran J, *J Bio Tribo Corros*, 5 (2019) 1.
15 Telegdi J, *Materials*, 13 (2020) 5089.
16 Prabakaran M, Kim S H, Kalaiselvi K, Hemapriya V & Chung I M, *J Taiwan Inst Chem Eng*, 1 (2016) 553.
17 Jyothi S, Rao Y S & Ratnakumar P S, *Rasayan J Chem*, 12 (2019) 537.
18 A l Maofaria A, Doucha S, Benmessaouda M, Hajjaji S E, Mosaddak M & Ouaki B, *Port Electrochimica Acta*, 39 (2021) 21.
19 Bayol E, Gürten A A, Dursun M & Kayakirilmaz K, *Acta Physico Chimica Sinica*, 24 (2008) 2236.
20 Africa S, *Afr J Pure Appl Chem, 2 (*2008) 46.
21 Graham D, *J Phys Chem*, 57 (1953) 665.
22 Li X, Deng S & Fu H, *Corros Sci*, 53 (2011) 1529.
23 E l Hamdani N, Fdil R, Tourabi M, Jama C & Bentiss F, Appl Surf Sci, 357 (2015) 1294.
24 Krishnaveni K & Ravichandran J, *T Nonferr Metal Soc*, 24 (2014) 2704.
25 Ibrahim S R, Mohamed G A, Khedr A I, Zayed M F, E l Kholy A A, *J Food Biochem*, 42 (2018) 12491.
26 My M & Ap S, *Int Food Res J*, 26 (2019) 1023.
27 Sudiarta I W, Saputra I W, Singapurwa N M, Candra I P & Semariyani A A, *J of Physic: Conference Series*, IOP Publishing, Bristol, United Kingdom. 1869 (2021) 012032.
28 Paśko P, Galanty A, Zagrodzki P, Luksirikul P, Barasch D, Nemirovski A & Gorinstein S, *Molecules*, 26(2021) 2158.